Thesis for the degree of Licentiate of Engineering
in
Machine and Vehicle Systems

Modeling and Analysis of Longitudinal Vehicle Dynamics Near Standstill with Brake Friction

Samira Deylaghian

Department of Mechanics and Maritime Sciences
CHALMERS UNIVERSITY OF TECHNOLOGY
Göteborg, Sweden 2026

Modeling and Analysis of Longitudinal Vehicle Dynamics Near Standstill with Brake Friction

Samira Deylaghian

Thesis for the degree of Licentiate of Engineering

Department of Mechanics and Maritime Sciences
Division of Vehicle Engineering and Autonomous Systems
Chalmers University of Technology
SE–412 96 Göteborg
Sweden
Telephone: +46 (0)31–772 1000

Chalmers Digitaltryck
Göteborg, Sweden 2026

“Everything should be made as simple as possible, but not simpler.”

— Albert Einstein

Modeling and Analysis of Longitudinal Vehicle Dynamics Near Standstill with Brake Friction

Samira Deylaghian
Department of Mechanics and Maritime Sciences
Chalmers University of Technology

Abstract

Longitudinal vehicle dynamics play a critical role in ride comfort at low speeds, particularly during frequent start-and-stop manoeuvres in everyday driving. Under such conditions, friction-induced dynamics and abrupt changes in acceleration can lead to significant jerk and passenger discomfort. This thesis investigates low-speed longitudinal dynamics with a focus on friction effects, non-smooth behavior, and near-standstill jerk.

A minimal vehicle model is developed to capture the essential longitudinal dynamics associated with propulsion, braking, and friction. To accurately represent transitions between static and dynamic friction, an event-driven numerical framework based on a state-machine formulation is introduced, enabling reliable simulation of stick–slip behavior and zero-velocity crossings. The non-smooth nature of the system is further analyzed using a Filippov framework, allowing phase-space investigation of motion near switching boundaries and providing insight into stability, trapping regions, and oscillatory behavior.

The modeling approach is supported by experimental measurements from a real vehicle test conducted on an inclined road using high-resolution IMU sensors. Experimental data are used for parameter estimation, torque reconstruction, and state estimation through a Kalman filter, enabling phase-space analysis of the relative motion between the vehicle body and wheel. Taken together, the numerical, analytical, and experimental results provide a coherent description of longitudinal vehicle dynamics at low-speed.

Keywords: Longitudinal dynamics, Low-speed driving, Experimental analysis, Jerk analysis, Discontinuous systems.

Acknowledgments

This work would not have been possible without the support of many people.

First and foremost, I would like to thank my supervisors, Mats Jonasson and Petri Piiroinen, for their guidance, patience, and continuous encouragement throughout this work. I am grateful for their valuable feedback, thoughtful discussions, and the trust they placed in me during the research process. I would also like to thank my examiner, Håkan Johansson, for his time and insightful comments throughout the project.

I would also like to acknowledge my colleagues at the Vehicle Engineering and Autonomous Systems (VEAS) division at Chalmers University of Technology. I truly appreciate the friendly and inspiring working environment, as well as the everyday support and discussions that made this journey both easier and more enjoyable.

My deepest gratitude goes to my parents, Maman Zahra and Baba Hamid, for their endless love and encouragement throughout my studies, and for always believing in me. I would also like to thank my brothers, Ali and Sajjad, for their constant support and motivation during this journey.

Finally, I would like to express my sincere thanks to my friends for their kindness, friendship, and support throughout this period. Their presence brought warmth and joy to my life and helped me recharge during weekends, making it easier to stay focused and motivated during the week. They made this time brighter and helped me feel at home. Special thanks go to Mandana and Homa, whose support and friendship made this time even more meaningful.

This thesis comprises a summary and is based on the following appended papers. The appended papers are identical in content to the published or submitted versions. Minor editorial modifications have been made to ensure consistency with the format and layout of the thesis.

Paper A
S. Deylaghian, M. Jonasson, P. T. Piiroinen, *"A comparative study of discomfort using electrical and friction braking at low-speed driving,"* 2024, *16th International Symposium on Advanced Vehicle Control (AVEC 2024)*, Lecture Notes in Mechanical Engineering, Springer, Cham, doi:10.1007/978-3-031-70392-8_101.

Paper B
S. Deylaghian, M. Jonasson, P. T. Piiroinen, *"State estimation and characterization of longitudinal vehicle dynamics at low speeds using experimental data,"* 2025, *29th IAVSD Symposium on the Dynamics of Vehicles on Roads and on Tracks (IAVSD 2025)*.

Paper C
S. Deylaghian, P. T. Piiroinen, M. Jonasson, *"Locating Trapping Regions and Analysing Jerk in a Minimal Vehicle Model,"*, Submitted to *International Journal of Non-Linear Mechanics*, 2026.

Table of Contents

Introductory Chapters

Chapter 1

Introduction

This chapter introduces the scope and motivation of the thesis, focusing on longitudinal vehicle dynamics and the challenges associated with braking, friction, and jerk near standstill. It outlines why low-speed manoeuvres are critical for ride comfort, modeling, and control, and motivates the need for analysis tools capable of capturing non-smooth dynamics. The chapter reviews the relevant background and motivation, followed by an overview of longitudinal dynamics, non-smooth dynamics, and friction. It then presents the problem definition and research questions, discusses the limitations, and concludes with an outline of the thesis structure.

1.1 Background and Motivation

A deep understanding of vehicle dynamics is fundamental for analyzing and improving vehicle behavior, enabling the optimization of performance, ride comfort, and control strategies. Low-speed longitudinal driving forms a significant part of everyday operation and commonly occurs during start–stop manoeuvres, traffic creeping, hill driving, parking, and traversal of uneven road surfaces. In such conditions, the longitudinal response is strongly influenced by external disturbances, road characteristics, and actuator behavior. As a result, even minor variations in applied propulsion torque or braking force can induce noticeable acceleration fluctuations, which are readily perceived by passengers and may lead to reduced ride comfort.

Several practical issues are particularly relevant close to standstill. During hill starts and hill stops, gravitational loading increases the sensitivity of the vehicle response and can amplify transients in acceleration. In these manoeuvres, imprecise stopping or unintended rollback may compromise position accuracy and safety. Moreover, when the wheel reaches zero speed, the vehicle body may continue to oscillate due to driveline and suspension compliance, meaning that the wheel can be stationary while the body motion is still settling. Such effects are often associated with friction phenomena in

the brake mechanism and at the tire–road interface, as well as mechanical compliance and backlash, all of which may introduce abrupt changes in longitudinal force and acceleration over very short time scales.

One of the most direct consequences of these abrupt fluctuations is the occurrence of jerk, defined as the rate of change in acceleration. Jerk has been consistently linked to motion comfort, as rapid changes in longitudinal acceleration are strongly perceived by the human body [1, 2]. De Winkel et al. [1] showed that both acceleration and jerk influence how strongly motion is perceived, highlighting the importance of jerk in evaluating ride comfort. In a later study, De Winkel et al. [2] further demonstrated through simulator experiments that discomfort increases with both acceleration amplitude and jerk intensity, and that this sensitivity depends on the magnitude and direction of the motion. At low speeds, where tire forces and brake dynamics dominate, even small torque fluctuations can induce pronounced jerk, affecting both ride comfort and the driver's ability to maintain precise control. From a safety perspective, excessive jerk can degrade braking stability and disturb stopping performance, particularly during near-standstill manoeuvres [3]. These findings underline the importance of limiting sudden changes in acceleration when evaluating or controlling low-speed longitudinal motion, where jerk becomes a dominant factor influencing the comfort experience.

In the present thesis, acceleration and jerk are employed as the main indicators for analysis of transient responses during braking and start–stop events. They provide a direct link between the underlying vehicle dynamics, perceived comfort, and control-related performance measures. The following sections introduce the theoretical background and modeling framework used to describe these phenomena, with emphasis on non-smooth friction effects and their influence on low-speed vehicle motion.

1.2 Longitudinal Dynamics

Understanding low-speed motion requires careful consideration of longitudinal vehicle dynamics, which describe motion along the direction of travel and play a central role in vehicle control, comfort, and safety [4]. While vertical dynamics have been extensively investigated due to their influence on ride quality and structural loading, longitudinal dynamics is equally important, particularly during acceleration and deceleration events. In addition, vertical vibrations induced by road unevenness can significantly influence the longitudinal response by introducing additional resistance forces and altering the vehicle's effective force response [5]. As a result, longitudinal motion cannot be regarded as independent of the vehicle's vertical dynamics. When suspension motion is considered, longitudinal dynamics becomes coupled with vertical and pitch motions of the vehicle body and wheels, affecting force transmission, vehicle speed variations, and energy dissipation, especially when the vehicle encounters uneven road profiles or surface irregularities [6]. Accounting for these interactions therefore provides a

more realistic description of vehicle behavior and improves the prediction of transient longitudinal responses under real driving conditions.

Experimental and simulation-based studies have further shown that low-speed start–stop scenarios remain challenging even with advanced longitudinal controllers, due to actuator limitations and transient force behavior near standstill [7]. These findings highlight the gap between control design and the underlying vehicle dynamics that govern longitudinal motion at very low speeds. A key contributor to this behavior is the tire–road interaction, which governs the generation and transmission of propulsion and braking forces. Variations in road friction play a particularly important role at low speeds where sudden changes, such as μ-step conditions (abrupt transitions between road surfaces with different friction coefficients), can induce pronounced transient responses in the longitudinal tire force, leading to oscillatory behavior and reduced vehicle stability [8].

As a consequence of these effects, modeling assumptions that are adequate for smooth operation at higher speeds often fail to capture the behavior observed as the vehicle approaches zero velocity. In this context, stick–slip phenomena and force discontinuities give rise to non-smooth, event-driven dynamics, for which conventional continuous modeling approaches become inadequate. This motivates a closer examination of non-smooth dynamic transitions and their implications for low-speed longitudinal motion, which is addressed in the next subsection.

1.2.1 Dynamic Analysis

Low-speed braking and traction manoeuvres often involve abrupt changes in the underlying system dynamics, leading to behaviors that cannot be described by smooth trajectories alone. These transitions are typically triggered by physical threshold events such as the onset of wheel slip, wheel locking during braking, activation of anti-slip functions, or changes in tire–road adhesion. Such phenomena result in discrete events in the dynamics, where the governing equations change from one mode of motion to another. As a consequence, the vehicle response may exhibit sharp variations in acceleration and velocity, which are particularly evident in stick–slip behavior during braking. These effects have been widely reported in studies of low-speed longitudinal vehicle motion, where conventional continuous models struggle to capture the oscillatory responses and velocity fluctuations observed near standstill [7].

Dynamic systems of this kind are frequently described as piecewise-smooth, meaning that the motion evolves according to different continuous vector fields in distinct regions of the state space. When a trajectory reaches a switching surface, such as the boundary between sticking and slipping, the system undergoes a discrete change in its governing equations, creating a non-smooth response [9]. In friction-driven systems, this can give rise to motion along the switching surface, a behavior that is characteristic of Filippov systems [10]. Such dynamics is highly relevant when analyzing braking

at low speeds, where stick–slip transitions play a dominant role in shaping the vehicle response and is one major source of jerk and motion irregularities.

Accurate analysis of such systems requires tools that can handle event-driven transitions and the discontinuities that arise at switching surfaces. Traditional methods for smooth dynamical systems may produce misleading results or fail to predict certain behaviors. To address this, event-detection techniques and non-smooth analysis frameworks are used to track transitions between modes and to accurately simulate motion on and across discontinuity boundaries. The numerical method proposed by Piiroinen and Kuznetsov [11] is one example of an event-driven approach that stabilizes trajectories near discontinuity surfaces and precisely locates entry and exit points on the discontinuity boundary.

Motivated by these considerations, and given that the present work focuses on low-speed braking where non-smooth transitions are fundamental, dynamic analysis based on piecewise-smooth and event-driven concepts is adopted. This perspective forms the basis for the modeling approach developed in Chapter 2, where the braking system is represented as a Filippov-type system to capture stick–slip dynamics and the associated transient responses.

1.2.2 Friction Brake

At low speeds, where tire–road interaction dominates over aerodynamic or inertial effects, precise control of propulsion and braking forces becomes essential to prevent undesirable transient responses, such as oscillatory motion and excessive jerk [5, 8]. However, the interaction between the brake system and the tire–road interface introduces complex behaviors which can strongly influence the vehicle response [7]. As a result, braking plays a decisive role in shaping low-speed longitudinal dynamics and has received significant attention in both experimental and modeling studies.

Existing studies have examined braking behavior under low-adhesion conditions [12], force responses during slip transitions [8], and regenerative braking strategies aimed at improving energy efficiency [13, 14]. These studies collectively show that braking performance and ride comfort are highly sensitive to friction variations and operating conditions, making accurate modeling essential for predicting and mitigating unwanted dynamic effects.

Building on these findings, several studies have focused on improving low-speed braking control by explicitly considering jerk as a measure of ride comfort. Lee and Choi [15] proposed a jerk-minimizing control strategy based on smooth acceleration trajectories, while Singh and Nishihara [16] incorporated tire–road friction into a minimum-jerk trajectory design to improve stopping stability. Although jerk-aware control can improve comfort, many existing models rely on smooth formulations that fail to capture stick–slip transitions and abrupt friction changes near standstill, often resulting in oscillatory or irregular motion.

A key physical mechanism during braking is dry friction at the tire–road interface. Depending on the applied brake force, the wheel may alternate between sticking and sliding, transitioning from static to kinetic friction once a force threshold is exceeded. Under these conditions, even small variations in brake torque may trigger stick–slip transitions, leading to irregular force transmission and increased sensitivity to external disturbances [8, 6]. These friction-driven effects strongly influence acceleration behavior and are a primary source of oscillations and jerk near standstill. Capturing these effects accurately therefore requires braking models that can represent friction-driven transitions without relying solely on smooth force approximations.

From a modeling standpoint, a variety of friction formulations have been proposed to represent stick–slip behavior. Reviews of dry friction force models highlight the differences between simple static formulations and more advanced dynamic models in terms of physical fidelity and numerical behavior [17]. Dynamic models such as the Dahl and LuGre models introduce internal state variables to capture presliding displacement, hysteresis, and smooth force evolution [18, 17]. While these models offer improved physical realism, they also increase modeling complexity and parameter sensitivity. The implications of these modeling choices for braking analysis are examined in detail in Chapter 2.

1.3 Problem Definition

Low-speed start–stop manoeuvres are strongly influenced by friction-driven transitions between sticking and sliding. These transitions introduce non-smooth behavior and may generate abrupt changes in acceleration and increase jerk. Capturing such effects is essential for analyzing ride comfort, position accuracy, and stability near standstill. However, many standard modeling approaches rely on smooth formulations that are not well suited to represent discontinuities and mode switching. Beyond the physical non-smoothness, low-speed operation also presents practical challenges for simulation and evaluation. Numerical integration may become unreliable if zero-velocity crossings and stick–slip transitions are not handled explicitly, and friction laws may introduce discontinuities that lead to solver sensitivity. In parallel, sensing and control at very low speeds are challenging because motion states become harder to estimate accurately. Standard sensors may provide limited resolution near zero velocity, and derivative-based quantities such as jerk are particularly sensitive to noise. Together, these aspects make low-speed manoeuvres challenging to model, simulate, and validate, motivating the need for modeling frameworks and numerical tools that can robustly capture non-smooth behavior arising from friction in this operating range.

1.3.1 Objective and Contributions

The main objectives of this work are:

- To analyze the dynamics of low-speed longitudinal motion, with emphasis on braking-induced non-smooth events.
- To develop a simplified model that captures friction-driven transitions and supports jerk-based motion analyses.
- To compare the model behavior against simulation results and vehicle measurements in order to assess model fidelity.
- To provide insight into the vehicle and friction dynamics that support the development of smoother and more predictable low-speed control strategies.

1.3.2 Research Questions

This thesis is guided by the following research questions:

RQ1: To what extent can a minimal longitudinal vehicle model represent real-world oscillation problems?

RQ2: Can a mathematical and computational framework be formulated that accounts for the non-smooth characteristics of braking systems and produces simulation results consistent with physical brake tests?

Each of the appended papers contributes to answering these questions, see Fig. 1.1. Paper A [19] investigates the dynamic behavior of a minimal longitudinal model through simulation, while Paper B [20] evaluates corresponding behavior through real-vehicle measurements, jointly addressing **RQ1**. Paper C [21] focuses on the analysis of a non-smooth numerical approach for braking dynamics, directly addressing **RQ2**. Together, these studies cover the problem from complementary perspectives, combining vehicle modeling, mathematical treatment of non-smooth dynamics, and experimental validation on a real vehicle. The combined outcome of these studies establishes a coherent framework for analyzing low-speed longitudinal motion with friction-induced non-smooth effects.

1.3.3 Limitations

This work focuses on low-speed longitudinal vehicle motion and therefore adopts a number of simplifying assumptions. Lateral and yaw dynamics are not considered, and steering effects are neglected. Aerodynamic drag and rolling resistance are neglected

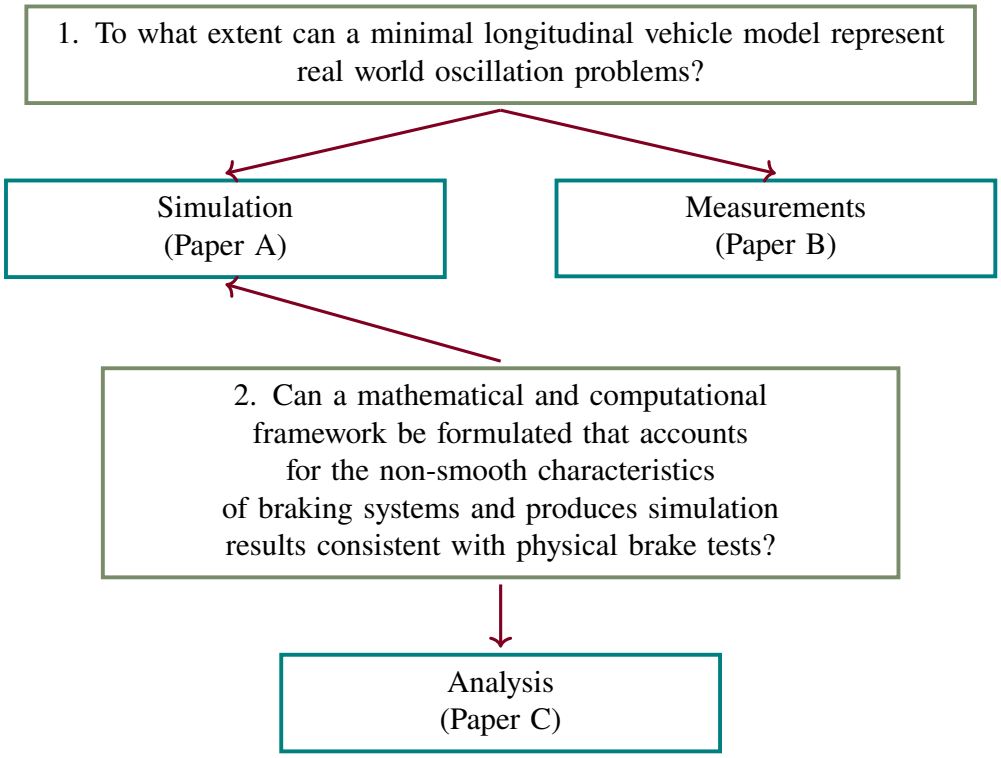

Figure 1.1: Overview of the research questions and appended papers.

in the minimal vehicle model, as their influence is assumed to be small in the low-speed operating range considered.

The tire–road interaction is represented through simplified friction models without explicit tire slip dynamics, detailed tre deformation effects, or contact patch modeling. The purpose of the friction formulation in this work is not to develop or identify new friction models, but to represent friction transitions. The vehicle model considers only a single wheel, and coordination effects between multiple wheels and actuators are therefore not addressed. In addition, mechanical effects such as suspension backlash and compliance are not explicitly modeled, and high-frequency dynamics are not included.

Furthermore, the experimental analysis is limited to longitudinal start and stop manoeuvres on a straight, inclined road, with no cornering, and does not cover more complex driving scenarios or varying road surface conditions. While these assumptions limit the generality of the results, they allow for a focused investigation of non-smooth behavior and jerk generation near standstill, which are the primary objectives of this study.

1.4 Structure of the Thesis

The remainder of this thesis is organized as follows. Chapter 2 presents the modeling framework used to describe low-speed longitudinal vehicle motion, including the formulation of the minimal vehicle model and the representation of braking friction. Chapter 3 focuses on the analysis of acceleration and jerk in the presence of non-smooth dynamics, introducing analytical jerk estimation for starting and stopping manoeuvres. Chapter 4 introduces the numerical methods applied to capture friction switches and stick–slip behavior. The experimental setup, test conditions, and data processing steps are described in Chapter 5. The resulting simulations, measurements, and comparative analyses are presented in Chapter 6, with particular emphasis on model fidelity and transient behavior. The findings are discussed and synthesized in Chapter 7, where the main conclusions are drawn and directions for future work are outlined.

Chapter 2

Modeling

To investigate the mechanisms governing low-speed longitudinal motion and the generation of jerk during start and stop manoeuvres, a simplified yet physically representative vehicle model is introduced in this chapter. The proposed model captures the essential dynamics associated with propulsion, braking, and tire–road friction, while remaining sufficiently simple to allow for analytical insight into transient behavior. By focusing on hill start and stop scenarios, where both driving and braking torques interact with frictional effects, the model provides a suitable framework for analyzing how different actuation strategies influence acceleration and jerk. This modeling approach forms the basis for the subsequent analysis of comfort-related dynamics and non-smooth behavior in low-speed vehicle motion.

2.1 Vehicle Model

A minimal longitudinal vehicle model is employed to capture the essential dynamics governing low-speed motion during start and stop manoeuvres. The model focuses on longitudinal dynamics near standstill, where oscillatory motion and rapid changes in acceleration are most pronounced. To balance physical realism with analytical simplicity, only the physical components and degrees of freedom necessary to capture these effects are included, avoiding model complexity. Therefore, the full vehicle is represented by a single equivalent wheel and a simplified suspension system, which is sufficient to describe the dominant longitudinal dynamics under the operating conditions considered in this study.

The model consists of three main components: a sprung mass representing the vehicle body with mass m_b, an unsprung mass representing the wheel hub with mass m_a, and a rigid wheel with mass m_w, radius r, and moment of inertia J. The wheel hub and the vehicle body are connected through a linear spring–damper element with spring stiffness k and damping coefficient d, which represents the combined longitudinal compliance of

the suspension and tire. This configuration allows relative longitudinal motion between the vehicle body and the wheel–hub assembly. A schematic representation of the model is shown in Fig. 2.1.

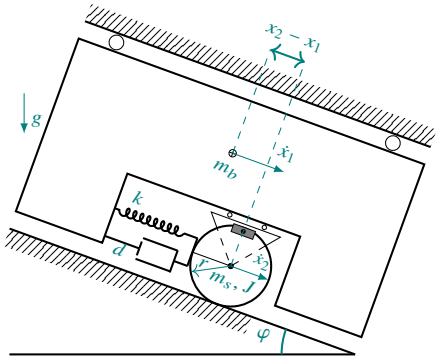

Figure 2.1: The minimal vehicle model.

To simplify the system, all four wheels are lumped into a single representative wheel. This assumption is motivated by the focus on low-speed longitudinal motion, where individual wheel dynamics and asymmetric effects have a limited influence. Secondary resistance forces such as aerodynamic drag and rolling resistance are neglected. This assumption is reasonable in low-speed scenarios, where such effects are small compared to propulsion, braking, and friction forces. The model is considered on a road with inclination angle φ, enabling the analysis of start and stop manoeuvres under gravitational loading. Pitch motion of the vehicle body is neglected, as the analysis is limited to straight-line low-speed manoeuvres where its influence on longitudinal dynamics is small.

The longitudinal motion of the system is described by two translational degrees of freedom: the displacement of the vehicle body x_1 and the displacement of the wheel hub x_2, both measured relative to the road surface. Their corresponding velocities and accelerations are denoted by $\dot{x}_1$, $\dot{x}_2$ and $\ddot{x}_1$, $\ddot{x}_2$, respectively. The wheel rotates with angular velocity ω and is subjected to a propulsion torque T_p and a friction brake force F_b. A no-slip condition between the tire and the road is assumed, leading to the kinematic constraint

$$\dot{x}_2 = r\omega. \tag{2.1}$$

Based on these assumptions, the equations of motion are derived from the free-body diagrams of the vehicle body and the wheel–hub assembly shown in Fig. 2.2, where all relevant longitudinal forces and torques are identified. The longitudinal interaction between the vehicle body and the wheel–hub assembly is represented by the spring–damper force F_a.

At the tire–road interface, the longitudinal tire force F_x transmits propulsion and braking forces to the road. This force is limited by the available friction according to

$$|F_x| \leq \mu_s F_N, \tag{2.2}$$

where F_N denotes the normal load and μ_s is the static road–tire friction coefficient. In the present work, explicit tire slip dynamics is not modeled. Instead, the friction limit is enforced implicitly through the braking force formulation and the associated stick–slip transitions. Under sticking conditions, the rolling constraint is satisfied and the longitudinal force adjusts to balance the applied torques, while sliding occurs when the friction bound is reached. Consequently, the effect of the longitudinal tire force enters the equations of motion through the friction and braking terms rather than as an independent force variable.

Figure 2.2(a) shows the vehicle body, represented by the sprung mass m_b. The body is subjected to the longitudinal suspension interaction force F_a and the component of gravity acting along the road slope. The forces F_e, T_v, and T_h, shown in the free-body diagram, represent the internal constraint forces and moments introduced by the auxiliary rollers used to guide the motion of the model and prevent vertical and rotational degrees of freedom. Specifically, F_e denotes the normal contact force between the wheel hub and the body, while T_v and T_h are the moments generated by the rollers.

These forces and moments do not perform work in the longitudinal direction and, therefore, do not contribute to the longitudinal dynamics considered here. Vertical motion and pitch dynamics are neglected, and a static equilibrium in the constrained directions is assumed. Applying Newton's second law of motion in the longitudinal direction thus yields

$$m_b \ddot{x}_1 = F_a + m_b g \sin\varphi. \tag{2.3}$$

The longitudinal spring–damper element connecting the vehicle body and the wheel–hub assembly is shown in Fig. 2.2(b). The interaction force transmitted between the two subsystems is modeled as a linear spring–damper relation,

$$F_a = k(x_2 - x_1) + d(\dot{x}_2 - \dot{x}_1). \tag{2.4}$$

The wheel–hub assembly is modeled by separating the unsprung subsystem into a wheel hub and a rigid wheel. The wheel hub (Fig. 2.2(c)) is acted upon by the suspension interaction force F_a, the longitudinal hub–wheel interaction force F_h, and the normal hub–wheel interaction force F_n. The rigid wheel (Fig. 2.2(d)) is driven by the propulsion torque T_p and opposed by the braking force F_b, while the tire–road contact provides the longitudinal ground reaction F_x and the normal load F_N.

By combining the longitudinal force balance of the hub with the rotational dynamics of the wheel about its center, the dynamics of the wheel–hub coordinate x_2 can be written as

$$\left(\frac{J}{r} + r\,(m_a + m_w)\right)\ddot{x}_2 = T_p - rF_b - rF_a + r\,(m_a + m_w)\,g\sin\varphi. \tag{2.5}$$

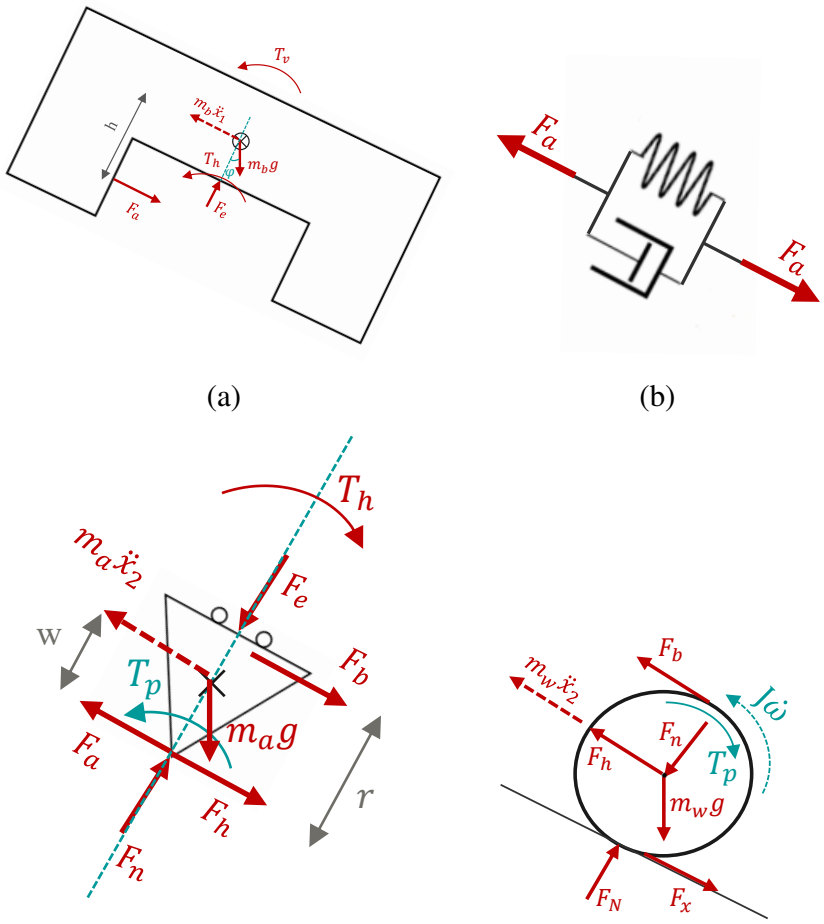

Figure 2.2: Free body diagram.

Combining the force and torque balances derived from the free-body diagrams, the resulting equations of motion for the system are given by

$$m_b\ddot{x}_1 = k(x_2 - x_1) + d(\dot{x}_2 - \dot{x}_1) + m_b g\sin(\varphi), \tag{2.6}$$

$$m_e\ddot{x}_2 = -k(x_2 - x_1) - d(\dot{x}_2 - \dot{x}_1) + m_s g\sin(\varphi) + \frac{T_p}{r} - F_b(\dot{x}_2), \tag{2.7}$$

where $m_s = m_a + m_w$ denotes the total unsprung mass. The effective mass m_e accounts for both translational and rotational inertia of the wheel and is defined as

$$m_e = \frac{J + r^2 m_s}{r^2}. \tag{2.8}$$

Equations (2.6)–(2.7) form a coupled set of equations of motion that govern the longitudinal dynamics of the vehicle body and the wheel–hub assembly. The formulation highlights how propulsion and braking torques interact with suspension forces, gravitational effects, and friction. In the following section, different friction models are reviewed with a focus on their ability to capture stick–slip behavior and non-smooth effects near standstill. Based on these analyses, a suitable nonlinear friction model is selected to define the braking force F_b used in this study.

2.2 Brake Friction Model

Friction is a dominant factor in low-speed longitudinal vehicle dynamics, particularly during braking and near-standstill manoeuvres where stick–slip transitions may occur. These transitions introduce non-smooth behavior into the system and are a primary source of sudden changes in acceleration and jerk. To accurately analyze such effects, appropriate friction models are required.

Different brake friction models have been proposed in the literature, differing in complexity, physical interpretation, and numerical properties. In this section, several commonly used friction models are reviewed to illustrate their qualitative behavior near zero velocity. The purpose of this comparison is not to develop a new friction formulation, but to assess which class of models is suitable for capturing friction transients relevant to low-speed while remaining compatible with the simplified vehicle model adopted in this study.

2.2.1 Static and Dynamic Friction Models

Friction models can be broadly classified into static (algebraic) models and dynamic models, depending on how the friction force is represented [17]. Static friction models describe the friction force as an explicit function of the instantaneous system states, typically velocity and normal force, without introducing additional internal dynamics. These models are simple to implement and computationally efficient, but they assume that friction responds instantaneously to changes in motion.

In contrast, dynamic friction models introduce internal state variables to represent the microscopic behavior of the contact interface, such as elastic deformation or bristle-like interactions between surfaces [17]. As a result, the friction force evolves dynamically and may depend on the history of motion rather than only the current velocity. This allows dynamic models to capture important phenomena such as presliding displacement, hysteresis, and smooth transitions during motion reversals.

The distinction between static and dynamic friction models becomes particularly important in low-speed applications. Near standstill, where velocity changes are small and frequent reversals occur, static models often lead to discontinuous force responses

and unrealistic acceleration or jerk predictions. Dynamic models provide a more physically meaningful description in this regime, but at the cost of increased modeling complexity and additional parameters. These differences motivate a careful evaluation of friction model formulations before their application to low-speed vehicle dynamics.

2.2.2 Coulomb Friction Model

The simplest representation of friction is the Coulomb friction model [17], where the friction force opposes motion with a magnitude proportional to the normal force. The friction force F_f is expressed as

$$F_f(v) = \begin{cases} [-\mu_s F_N, \mu_s F_N], & v = 0, \\ \mu_d F_N \operatorname{sign}(v), & v \neq 0, \end{cases} \tag{2.9}$$

where μ_s and μ_d denote the static and dynamic friction coefficients, respectively, F_N is the normal force, and v denotes the relative sliding velocity.

The Coulomb friction model captures basic sticking and sliding behavior and provides a clear distinction between static and dynamic friction regimes. In this formulation, the friction force is an explicit function of the instantaneous velocity, and the model therefore belongs to the class of static friction models. However, it assumes an instantaneous transition between these regimes and does not account for velocity-dependent effects, presliding displacement, or smooth force variation near zero velocity. As a result, the model often produces discontinuous force responses that can lead to numerical difficulties and unrealistic acceleration and jerk predictions in low-speed simulations.

To overcome these limitations, velocity-dependent friction formulations incorporating the Stribeck effect have been introduced. These models provide a smoother transition between static and dynamic friction.

2.2.3 Dynamic Friction Models

In the following, two commonly used dynamic friction models are briefly introduced.

Dahl Friction Model

The Dahl friction model introduces an internal state variable that represents elastic deformation at the contact interface. Originally proposed to describe frictional damping and presliding behavior, the model captures frictional hysteresis and smooth force evolution during motion reversals, which are essential features of stick–slip dynamics. A key characteristic of the Dahl model is that the friction force evolves as a function of relative displacement rather than instantaneous velocity, allowing it to represent frictional lag effects that are not captured by static friction models [18].

In the Dahl formulation, the friction force is expressed as

$$F_f = \sigma_0 z, \tag{2.10}$$

where z denotes the internal friction state associated with elastic deformation at the contact interface, and σ_0 represents the corresponding contact stiffness that scales the elastic friction force. The evolution of this internal state is governed by

$$\dot{z} = v - \frac{|v|}{F_{st}} z, \tag{2.11}$$

with v denoting the relative sliding velocity and F_{st} representing the steady-state friction force.

The model exhibits smooth transitions during velocity reversals and captures presliding displacement, making it well suited for analyzing friction-induced oscillations and non-smooth behavior in low-speed mechanical systems.

LuGre Friction Model

Another widely used dynamic friction model is the LuGre model [17], which extends the Dahl formulation by representing the friction interface as an ensemble of microscopic bristles with elastic and damping properties. The model introduces an internal state variable that describes the average bristle deflection, allowing it to capture presliding displacement, frictional hysteresis, the Stribeck effect, and viscous friction contributions within a unified framework.

In the LuGre formulation, the friction force is expressed as

$$F_f = \sigma_0 z + \sigma_1 \dot{z} + \sigma_2 v, \tag{2.12}$$

where z denotes the internal friction state, v is the relative sliding velocity, and σ_0, σ_1, and σ_2 represent the bristle stiffness, micro-damping, and viscous damping coefficients, respectively. The evolution of the internal state is governed by

$$\dot{z} = v - \sigma_0 \frac{|v|}{g(v)} z, \tag{2.13}$$

where the function $g(v)$ accounts for the Stribeck effect by describing the transition between static and dynamic friction regimes.

The LuGre model provides a rich physical interpretation and captures a wide range of friction phenomena observed near zero velocity. However, the introduction of additional states and parameters increases modeling complexity and complicates parameter identification and numerical simulation. For applications focused on low-speed vehicle dynamics and jerk analysis, this added complexity may limit its practical usefulness compared to simpler velocity-dependent friction formulations.

2.2.4 Benson Friction Model

Based on the requirements of this study, a friction formulation based on the Benson model is selected for the present work. The primary motivation for this choice is to capture stick–slip transitions and non-smooth behavior near standstill while maintaining a simple, intuitive, and numerically efficient model structure that is compatible with the minimal vehicle model adopted in this work.

The Benson model extends the classical Coulomb friction formulation by incorporating the Stribeck effect through a smooth exponential transition between static and dynamic friction regimes [17]. The Stribeck effect describes the reduction of friction force as relative velocity increases from zero, reflecting changes in the contact interface during motion initiation. In the Benson formulation, this behavior is captured by a velocity-dependent exponential term that ensures a gradual decay of friction from the static to the dynamic level without introducing additional internal states. Compared to more complex dynamic friction models, such as the LuGre model, the Benson formulation requires fewer parameters and is easier to interpret and implement.

The braking force is expressed as

$$F_b(\dot{x}_2) = \begin{cases} [-\mu_s F_c, \mu_s F_c], & \dot{x}_2 = 0, \\ \left(\mu_d + (\mu_s - \mu_d) e^{-(|\dot{x}_2|/v_s)^{\alpha}}\right) \operatorname{sign}(\dot{x}_2) F_c, & \dot{x}_2 \neq 0, \end{cases} \tag{2.14}$$

where F_c is the brake clamping force, v_s is the Stribeck velocity, and α controls the sharpness of the transition between friction regimes in the context of this thesis.

Although the Benson friction model does not include internal friction states, it captures the key phenomena relevant to low-speed longitudinal motion, including stick–slip transitions and velocity-dependent friction. Compared to dynamic friction models, it requires fewer parameters and offers a clearer physical interpretation, simplifying both analysis and implementation. In addition, dynamic friction models with internal states often require very small integration step sizes and careful parameter tuning, which can increase computational cost without providing additional benefit for the low-speed phenomena considered here. This balance makes the Benson model well suited for studying non-smooth friction effects and jerk behavior in low-speed vehicle dynamics.

2.3 Dynamical System Representation

Low-speed longitudinal motion with friction brakes involves changes in system behavior that cannot be described by a single smooth set of equations. In particular, transitions between wheel rolling and sticking introduce switching between different dynamic modes and lead to non-smooth system responses. To capture these effects in a consistent way, the vehicle dynamics in this thesis are formulated within a piecewise-smooth dynamical systems framework.

2.3.1 Filippov System

The friction model employed in this work leads to a system whose dynamics are governed by different smooth vector fields depending on the sign of the wheel velocity (see (2.14)). Such systems belong to the class of *Filippov systems* [9], which are characterized by state-dependent switching between vector fields across a discontinuity surface, with the governing ordinary differential equations (ODEs) being smooth within each region of the state space. Locally, the system dynamics are described by smooth ordinary differential equations within separate regions of the state space, while non-smooth behavior arises at the interfaces between these regions.

Let the system state be denoted by $z \in \mathbb{R}^n$, and let a scalar switching function $h(z)$ partition the state space into two regions,

$$S^+ = \{z \in \mathbb{R}^n \mid h(z) > 0\}, \tag{2.15}$$

$$S^- = \{z \in \mathbb{R}^n \mid h(z) < 0\}, \tag{2.16}$$

separated by the switching surface

$$\Sigma = \{z \in \mathbb{R}^n \mid h(z) = 0\}. \tag{2.17}$$

Within each region, the system evolves according to a smooth vector field, while transitions between regions occur when trajectories reach Σ.

In frictional systems, the behavior on the switching surface plays a crucial role. Depending on the orientation of the vector fields relative to Σ, trajectories may cross the surface or remain constrained to it. In the latter case, the system exhibits *sliding motion* in the Filippov sense, which requires an event-driven treatment to accurately capture entry, persistence, and exit from the switching surface [11]. In mechanical systems with dry friction, such sliding corresponds physically to *sticking*, where relative motion is constrained by friction forces.

To describe the dynamics on the switching surface, Utkin's equivalent control method is adopted [22]. This approach defines a vector field on the sliding surface as a convex combination of the adjacent vector fields, ensuring that trajectories remain confined to the surface while satisfying the governing equations of motion. This formulation provides a consistent way to describe constrained motion during sticking phases without introducing artificial regularization.

The minimal longitudinal vehicle model introduced earlier can be naturally embedded within the Filippov framework. The switching condition is defined by the wheel velocity, such that the switching surface corresponds to zero wheel speed. Away from this surface, the wheel is rolling and the dynamics are governed by smooth equations of motion. When the wheel velocity reaches zero, the system may enter a sticking regime, where motion is constrained by the friction brake.

By reformulating the second-order equations of motion as a first-order state-space system, the dynamics can be expressed as a piecewise-smooth system with velocity-dependent switching [21]. The resulting formulation clearly separates rolling and sticking regimes and enables a precise characterization of transitions between them. The sticking region on the switching surface is determined by the balance between elastic forces, damping, gravitational loading, and the maximum available static friction.

This dynamical systems representation forms the foundation for the numerical and analytical investigations carried out in subsequent chapters. In particular, it enables rigorous treatment of stick–slip transitions, supports event-based numerical integration, and provides a consistent framework for analyzing acceleration and jerk behavior near standstill.

Chapter 3

Acceleration and Jerk of the Minimal Model

Low-speed longitudinal motion is characterized by abrupt changes in acceleration arising from friction transitions and stick–slip behavior, which directly give rise to pronounced jerk near standstill. In such conditions, jerk becomes a key quantity for assessing transient vehicle response, ride comfort, and motion smoothness. Understanding how acceleration and jerk evolve during friction-driven transitions is therefore essential for analyzing low-speed start and stop maneuvers.

This chapter focuses on the numerical estimation of acceleration and jerk in the minimal longitudinal vehicle model introduced earlier. Starting from the governing equations of motion, expressions for the initial jerk associated with friction transitions are derived for the starting scenario. The analysis highlights how model parameters, braking inputs, and friction characteristics influence jerk generation.

3.1 Jerk Estimation

The jerk response of the system, defined as the time derivative of acceleration, is evaluated by analyzing the time evolution of the governing equations of motion introduced in Chapter 2. For analytical tractability, the model is simplified by neglecting the Stribeck effect in the braking force $F_b(\dot{x}_2)$, which is treated as a piecewise constant or linear function. This assumption is applied consistently throughout this chapter.

The starting case is considered, where motion is initiated from rest due to a step change in propulsion torque. The analysis considers a vehicle located on a fixed inclined road, and the road slope φ is assumed to remain constant during motion. The wheel is assumed to be initially at rest at $t = 0^-$, with the friction brake engaged. Motion is initiated at $t = 0^+$ due to an applied step input in the propulsion torque.

In this analysis, a simplified modeling approach is adopted:

- The Stribeck effect is neglected. Therefore, the braking force at the start of motion is taken as a constant value corresponding to dynamic friction, i.e.,

$$F_b(0^+) = \mu_d F_c. \tag{3.1}$$

- The propulsion torque T_p is modeled as a step input applied at $t = 0^+$.

According to Newton's second law of motion, a finite force can induce an instantaneous change in acceleration, whereas changes in velocity and position require finite time, since velocity and position are obtained as time integrals of acceleration and velocity, respectively. Consequently, at the instant of the friction transition, position and velocity remain continuous, while acceleration may change discontinuously.

Accordingly, the following initial conditions hold immediately after the transition

$$x_2(0^+) - x_1(0^+) = -\frac{m_b g \sin\varphi}{k}, \tag{3.2}$$

$$\dot{x}_2(0^+) = \dot{x}_1(0^+) = 0. \tag{3.3}$$

The objective is to compute the jerk at $t = 0^+$, i.e., the moment immediately after the friction transition. Substituting the initial conditions in (3.2) and (3.3) into the body equation (2.6), the body acceleration at the start of motion is obtained as

$$\ddot{x}_1(0^+) = 0. \tag{3.4}$$

Rather than analyzing the two equations of motion separately, equations (2.6) and (2.7) are combined, resulting in a single equation that describes the overall system dynamics, namely,

$$m_b\ddot{x}_1 + m_e\ddot{x}_2 = (m_s + m_b)g\sin\varphi + \frac{T_p}{r} - F_b(\dot{x}_2). \tag{3.5}$$

Substituting this result into the total system equation (3.5), the initial acceleration of the wheel becomes

$$\ddot{x}_2(0^+) = \frac{(m_s + m_b)g\sin\varphi + \frac{T_p(0^+)}{r} - F_b(0^+)}{m_e} \tag{3.6}$$

Differentiating (2.7) with respect to time and substituting the initial conditions together with the initial wheel acceleration given by (3.6) yields the wheel jerk

$$\dddot{x}_2(0^+) = -\frac{d}{m_e^2}\left((m_s + m_b)g\sin\varphi + \frac{T_p(0^+)}{r} - F_b(0^+)\right) - \frac{\frac{\dot{T}_p(0^+)}{r} - \dot{F}_b(0^+)}{m_e}. \tag{3.7}$$

Under the current assumptions:

- T_p is a step input, hence $\dot{T}_p(0^+) = \delta(t)$ which is non-zero only at $t = 0$, and zero elsewhere.
- F_b is constant at $\mu_d F_c$, so $\dot{F}_b(0^+) = 0$.

the expression for the wheel jerk at $t = 0^+$ simplifies to

$$\dddot{x}_2(0^+) = -\frac{d}{m_e^2}\left((m_s + m_b)g\sin\varphi + \frac{T_p(0^+)}{r} - \mu_d F_c\right). \tag{3.8}$$

Similarly, using the total system dynamics in equation (3.5), the body jerk at the onset of motion is given by

$$\dddot{x}_1(0^+) = \frac{d}{m_b m_e}\left((m_s + m_b)g\sin\varphi + \frac{T_p(0^+)}{r} - \mu_d F_c\right). \tag{3.9}$$

Several observations can be made from the jerk expressions in equations (3.8) and (3.9). First, the jerk magnitude scales linearly with the damping coefficient d, indicating that higher longitudinal damping leads to larger jerk amplitudes at the instant of the friction transition. In contrast, the stiffness parameter k does not appear in the jerk expressions, showing that the spring stiffness does not influence the instantaneous jerk response. This highlights that jerk is governed by force discontinuities and damping rather than elastic effects.

Furthermore, the jerk expressions exhibit an inverse dependence on the masses m_b and m_e, implying that smaller body or wheel masses result in higher jerk amplitudes. In the limiting case where either mass approaches zero, the jerk magnitude increases without bound, revealing a singular behavior that emphasizes the sensitivity of jerk to mass distribution in the minimal model.

By expressing the braking force as $F_b(0^+) = \mu_d F_c$ and noting that the applied torque $T_p(0^+)$ must exceed the static friction threshold $\mu_s F_c$ to initiate motion, the jerk expressions can be rewritten explicitly in terms of the static and dynamic friction coefficients,

$$\dddot{x}_2(0^+) = -\frac{d}{m_e^2}\left((m_s + m_b)g\sin\varphi + \frac{T_p(0^+)}{r} - \mu_s F_c + \Delta\mu F_c\right). \tag{3.10}$$

$$\dddot{x}_1(0^+) = \frac{d}{m_b m_e}\left((m_s + m_b)g\sin\varphi + \frac{T_p(0^+)}{r} - \mu_s F_c + \Delta\mu F_c\right), \tag{3.11}$$

where $\Delta\mu = \mu_s - \mu_d$ denotes the friction contrast between static and dynamic regimes.

This representation shows that higher values of $\Delta\mu$ lead to larger force discontinuities at the friction transition and therefore higher jerk. A similar effect is obtained by increasing the applied propulsion torque T_p, which also increases the force at the transition and will increase the resulting jerk. This behavior is consistent with the findings reported in Paper A, where an increase in the friction contrast at motion onset was shown to result in higher jerk amplitudes.

Chapter 4

Numerical Methods

The analysis of low-speed vehicle dynamics presented in this work involves discontinuities and non-smooth phenomena arising from frictional interactions and stick–slip transitions. Standard numerical integration techniques, when applied directly to such systems, may suffer from convergence issues, chattering, or inaccurate predictions of acceleration and jerk near zero velocity. To ensure robust and reliable simulation results, specialized numerical strategies are therefore required.

This chapter presents the numerical methods employed to handle the non-smooth nature of the friction model and the resulting state-dependent dynamics. In particular, a state-machine formulation is introduced to represent transitions between static and dynamic friction regimes, together with event-detection mechanisms that govern switching between these states. The chapter also describes the numerical solver setup and implementation details used to accurately capture transient behavior during low-speed motion. All numerical implementations were carried out in MATLAB. The event-driven integration scheme used to handle sliding motion in Filippov systems is based on the framework developed in [11]. This implementation was adapted and extended to incorporate the friction state machine and the specific structure of the minimal longitudinal vehicle model considered in this thesis.

4.1 State Machine

Accurate numerical simulation of frictional contact at low speeds is challenging due to discontinuities introduced by sign functions and abrupt transitions between sticking and sliding (see (2.14)). In particular, direct implementation of friction laws using the $\operatorname{sign}(\cdot)$ operator can lead to numerical chattering and unreliable predictions of acceleration and jerk near zero velocity. To address these issues, a state-based formulation of the friction force is adopted in this work.

Several state-machine formulations were initially explored to represent the transition

between static and dynamic friction. Based on numerical robustness and physical interpret ability, a three-state friction model was ultimately selected. In this formulation, the friction behavior is governed by a discrete state variable that can take the values $+1$, 0, or -1. These states correspond to motion in the positive direction, static friction (sticking), and motion in the negative direction, respectively.

The static state (0) represents a sticking condition, where the relative velocity is zero and the friction force adjusts to balance the external longitudinal forces acting on the system. In this state, the friction force is equal to the applied external force, as long as its magnitude remains within the admissible static friction bounds. When the magnitude of the external force exceeds the maximum static friction force, the system can no longer remain at rest and transitions to a dynamic state, i.e., it starts to move.

Transitions from the static state occur when the external force exceeds the static friction threshold. If the magnitude of external force becomes larger than the maximum static friction force in the positive direction, the system transitions from state 0 to state $+1$, corresponding to forward motion. Conversely, if the magnitude of external force exceeds the static friction limit in the negative direction, the state changes from 0 to -1, corresponding to backward motion. In the context of the vehicle model considered here, the external forces consist primarily of propulsion torque, inertia forces, and gravitational effects due to road slope.

When the system is in a dynamic state ($+1$ or -1), the friction force is governed by the dynamic friction model and has a constant magnitude that depends on the dynamic friction coefficient. During dynamic motion, a transition back to the static state may occur if the external force magnitude drops below the static friction threshold while the relative velocity approaches zero. In this case, the system enters the static state and the friction force once again balances the external force to maintain zero velocity.

Additionally, direct transitions between the two dynamic states are possible. For example, when the system is moving in the positive direction (state $+1$), a sufficiently large external force in the opposite direction may cause the friction force to reverse sign without sticking occurs, resulting in a direct transition to state -1. An analogous transition may occur from state -1 to state $+1$ under reversed loading conditions.

This three-state friction state machine enables a clear and numerically stable representation of stick–slip behavior and direction-dependent friction forces. By explicitly separating static and dynamic regimes and controlling transitions between them, the formulation avoids discontinuities associated with sign functions and provides reliable acceleration and jerk predictions during low-speed motion. A schematic illustration of the state transitions is provided in Fig. 4.1.

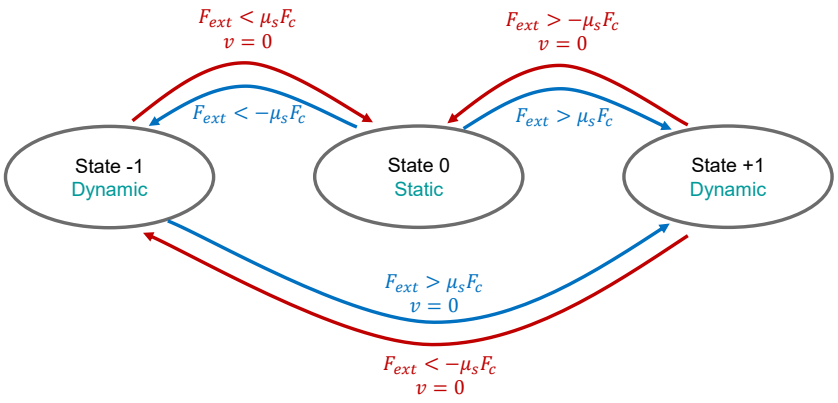

Figure 4.1: Friction state machine.

4.2 Event Function

To accurately capture transitions between static and dynamic friction regimes, an event function is employed during numerical integration. The role of this function is to detect physically significant conditions, such as velocity zero-crossings and violations of the static friction limits, and to trigger state transitions in the friction model accordingly.

In low-speed motion near standstill, these transitions strongly influence the system response. Without explicit event detection, numerical solvers may step over zero velocity or delay friction state changes, leading to inaccurate predictions of stopping time, friction force, and transient quantities such as acceleration and jerk.

In the present implementation, the event function is primarily used to detect velocity zero-crossings, which indicate potential transitions between dynamic motion and sticking. When such a condition is detected, the numerical solver terminates the current integration step and updates the friction state before continuing the simulation. This ensures that the system enters the static friction regime at a physically meaningful instant and prevents nonphysical oscillations around zero velocity.

By enforcing state transitions at well-defined event times, the event function improves numerical stability and ensures consistent handling of stick–slip behavior. As a result, the simulated friction force, acceleration, and jerk more accurately represent the system behavior during low-speed motion, especially near standstill.

4.3 Numerical Solver Setup and Implementation

The numerical setup of the vehicle model is performed using a coupled structure in which the vehicle dynamics, friction model, state machine, and event detection interact at each step. The friction behavior is evaluated in a state-machine and updated dynamically

based on the system response.

At a given time instant, the current system states, including displacement, velocity, and the friction state, are used to evaluate the friction force. This force is then supplied to the vehicle dynamics model, which computes the corresponding acceleration according to the governing equations of motion. The acceleration is integrated by the numerical solver to update the velocity and displacement states.

During integration, the event function continuously monitors the system for velocity zero-crossings. When such an event is detected, the solver terminates the current integration step and the friction state is updated according to the state-machine logic described in Section 3.1. Depending on the external forces acting on the system, the friction state may transition between static and dynamic regimes, or between forward and backward motion. After the state update, the integration is restarted with the updated friction state.

This structure ensures a consistent coupling between the continuous vehicle dynamics and the discrete friction state transitions. By explicitly separating friction evaluation, state updates, and numerical integration, the implementation avoids numerical chattering and nonphysical oscillations near zero velocity. As a result, the solver is able to robustly capture stick–slip behavior and produce reliable acceleration and jerk responses during low-speed motion.

Chapter 5

Real World Vehicle Testing

This chapter presents the experimental study conducted to investigate low-speed longitudinal vehicle dynamics under real driving conditions [20]. The experiments were designed to validate and complement the modeling and numerical analysis introduced in the previous chapters by providing measured data from a real vehicle maneuver.

Low-speed start and stop maneuvers were selected due to their frequent occurrence in everyday driving conditions. By combining inertial measurements with a minimal vehicle model and state estimation, the experimental study enables a detailed analysis of longitudinal dynamics and comfort-related quantities during near-standstill motion.

The chapter first describes the experimental setup, including instrumentation and test conditions. This is followed by an overview of the test maneuver and data pre-processing steps. Parameter estimation, state estimation, and analysis of the experimental results are then presented in subsequent sections.

5.1 Experimental Setup

This section describes the experimental setup used to investigate low-speed longitudinal vehicle dynamics. The focus is on real-world start and stop manoeuvres, which frequently occur in everyday driving and are particularly relevant for studying transient effects such as oscillations, relative motion between vehicle components, and jerk. Details of the test vehicle, instrumentation, and the experimental manoeuvre are provided in the following subsections.

5.1.1 Test Vehicle and Sensors

The experimental study was conducted using a Volvo XC40 equipped with its standard production suspension and braking systems. No modifications were made to the vehicle, ensuring that the measured responses reflect realistic driving conditions.

Two inertial measurement units (IMUs), Muse 221e [23], were installed on the vehicle to capture longitudinal dynamics. The sensors were operated at the same sampling rate and synchronized to ensure consistent timing between measurements. Both IMUs were configured to record data at a sampling frequency of 1600 Hz, providing sufficient temporal resolution to capture rapid transients associated with low-speed motion and jerk.

One IMU was mounted on the vehicle hood to measure longitudinal body acceleration. After gravity compensation and bias correction, this signal represents the second derivative of the vehicle body displacement. The second IMU was mounted at the center of the right front wheel hub to measure angular velocity. Using the known tire radius and assuming no tire slip, the angular velocity was converted to the wheel's translational speed.

This sensor configuration enables simultaneous observation of vehicle body motion and wheel dynamics, which is essential for analyzing relative motion, transient responses, and comfort-related quantities during low-speed driving.

5.1.2 Maneuver Design (Start and Stop)

The experimental manoeuvre was designed to excite longitudinal vehicle dynamics at low speeds while remaining simple and repeatable. Each test consisted of a start from rest, a short period of low-speed forward motion, and a controlled stop.

The vehicle was positioned on an uphill asphalt road to introduce a constant longitudinal gravitational load. Motion was initiated by releasing the brake system using the Auto Hold function and gradually increasing the accelerator pedal input, after which the vehicle moved forward at low speed for a short duration. The driver then manually applied the brake to bring the vehicle to a complete stop.

This manoeuvre reflects common real-world driving situations such as hill starts, traffic creeping, and parking. It also allows observation of key dynamic features, including the delay between wheel and body motion at start, oscillatory behavior of the suspension system, and the transient dynamics that occur as the vehicle approaches standstill.

5.2 Data Collection

During each test, acceleration and angular velocity were recorded continuously from both IMUs throughout the manoeuvre. The data sets consists of longitudinal body acceleration and angular velocity of the wheel, measured during repeated start and stop manoeuvres. These signals are used as the basis for signal processing, parameter estimation, and state estimation in the following sections.

5.3 Data Pre-Processing

Raw IMU measurements contain sensor noise, bias, and components unrelated to the longitudinal dynamics of interest. Therefore, several pre-processing steps were applied prior to analysis.

A zero-phase Butterworth low-pass filter [24] was applied to the measured signals to remove high-frequency noise while preserving the dominant motion-related dynamics. The cutoff frequency was selected based on frequency-domain analysis, which showed that the relevant longitudinal dynamics are concentrated at low frequencies. In addition, a notch filter [25] was used to suppress narrow-band disturbances associated with engine-related vibrations.

The measured body acceleration was corrected for bias and gravitational components arising from pitch motion. Vehicle body velocity was obtained by numerical integration of the filtered acceleration signal, with drift mitigation achieved through offset correction and trend removal. The angular velocity of the wheel was converted to translational wheel speed using the tire radius.

These processing steps ensure that the resulting signals accurately represent the physical motion of the vehicle and are suitable for further analysis.

5.4 State Estimation with Kalman filter

Although acceleration and wheel speed were directly measured, important quantities such as relative displacement between the vehicle body and the wheel, as well as wheel torque, are not directly observable. Moreover, direct numerical integration of acceleration signals to obtain displacement is prone to drift and noise amplification.

To address these limitations, a model-based state estimation approach was employed using a Kalman filter [26]. The filter combines the processed sensor measurements with the minimal vehicle model to estimate the full state vector, including the relative displacement and the relative velocity between the body and the wheel.

The Kalman filter operates by predicting the system state using the model dynamics and correcting this prediction based on incoming measurements. This approach provides physically consistent state estimates while reducing the influence of measurement noise. The resulting state estimates are used for phase-space analysis and jerk evaluation during start and stop manoeuvres.

Chapter 6

Results

This chapter presents the results obtained from numerical simulations and vehicle-level reference simulations, as well as experimental observations. The focus is on evaluating the ability of the proposed minimal model to reproduce low-speed longitudinal vehicle behavior and transient responses during start and stop manoeuvres. Particular attention is paid to velocity, acceleration, and jerk characteristics, which are central to ride comfort and control performance at low speeds.

6.1 Comparison of Simulation and CarMaker Results

To evaluate the capability of the proposed minimal longitudinal model, the simulation results were compared with reference simulations obtained from CarMaker [27]. The comparison focuses on vehicle velocity and longitudinal acceleration during a low-speed start and stop manoeuvre, as shown in Fig. 6.1.

The left side of the figure illustrates the simulation framework, where propulsion torque T_p and braking torque T_{brk} inputs extracted from the CarMaker model are applied as open-loop inputs to the Simulink implementation of the minimal vehicle model. The resulting body velocity V_x and acceleration Acc from the Simulink model are then compared directly with the corresponding CarMaker outputs.

The velocity comparison shows that the minimal model captures the overall motion profile well, including the initial acceleration phase, the peak velocity, and the subsequent deceleration towards standstill. Some deviations are observed near the velocity peak and during the stopping phase. These differences can partly be attributed to differences in damping behavior, where one system exhibits a more overdamped response while the other appears underdamped. Furthermore, the presence of an active controller in the CarMaker model may contribute to the observed discrepancies. In addition, the damping coefficients are difficult to tune consistently, as they cannot be directly accessed or identified from CarMaker, and it may not be realistic to represent all damping

effects using a single equivalent parameter. Another source of deviation is the absence of explicit tire–road friction modeling in the minimal model, which can influence the deceleration behavior. Finally, open-loop torque injection typically leads to velocity drift that increases over time. Despite these simplifications, the minimal model is still able to reproduce a qualitatively similar response. A similar level of agreement is observed in the acceleration comparison, where the timing and magnitude of the main acceleration and deceleration events are reasonably well captured. However, sharper acceleration peaks are observed in the CarMaker results, particularly during the initial start-up and braking phases. These effects are expected, as CarMaker includes detailed representations of tire dynamics, actuator behavior, and drivetrain compliance, which are intentionally neglected in the simplified model. Moreover, differences in vehicle mass and the inability to directly interpret the applied brake torque from CarMaker may further contribute to the observed discrepancies, highlighting the importance of validating the models against experimental data.

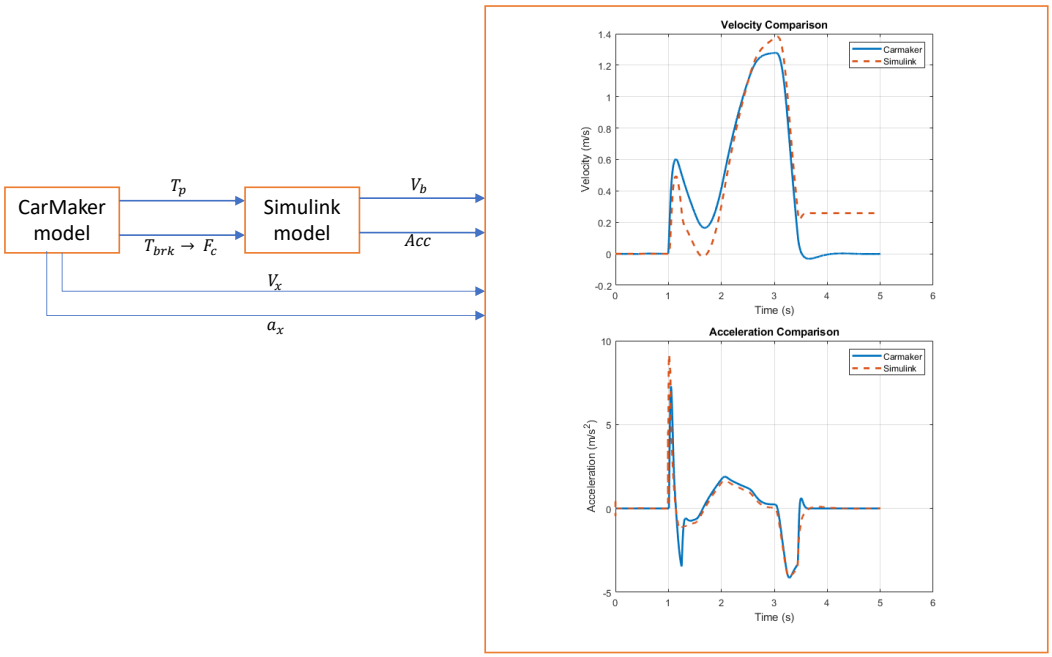

Figure 6.1: Comparison between CarMaker and Simulink results.

Overall, the comparison indicates that the minimal longitudinal model is able to reproduce the dominant low-speed dynamic behavior observed in CarMaker while maintaining a significantly lower model complexity. Despite known simplifications and parameter uncertainties, the model captures the essential transient characteristics, making it suitable for analyzing start–stop responses, jerk behavior, and non-smooth dynamics in low-speed manoeuvres.

6.2 Numerical and Experimental Observations

This section presents key observations from numerical simulations and experimental measurements, focusing on body jerk during low-speed start and stop manoeuvres. The section then examines the corresponding experimental data, phase-space representations, and wheel dynamics near standstill to characterize non-smooth behavior.

6.2.1 Body Jerk in Low-Speed Start-Stop Maneuvers

Figure 6.2 [19] shows the maximum body jerk during low-speed start and stop manoeuvres for different combinations of the static and dynamic brake friction coefficients, μ_s and μ_d. During vehicle start, Fig. 6.2(a) shows that body jerk increase markedly for higher values of the static friction coefficient μ_s and lower values of the dynamic friction coefficient μ_d. For all cases, motion initiation is associated with a pronounced jerk peak, whose magnitude depends on the friction parameters. The results indicate that larger μ_s combined with smaller μ_d lead to higher jerk levels during start. In contrast, the stopping behavior shown in Fig. 6.2(b) exhibits a different sensitivity to the friction parameters. After the wheel has reached zero velocity, the body jerk remain largely insensitive to variations in μ_s, while changes in μ_d have a clear influence. For a fixed μ_d, the jerk and acceleration levels remain nearly constant even when μ_s is varied, whereas increasing μ_d results in higher jerk and acceleration during stopping.

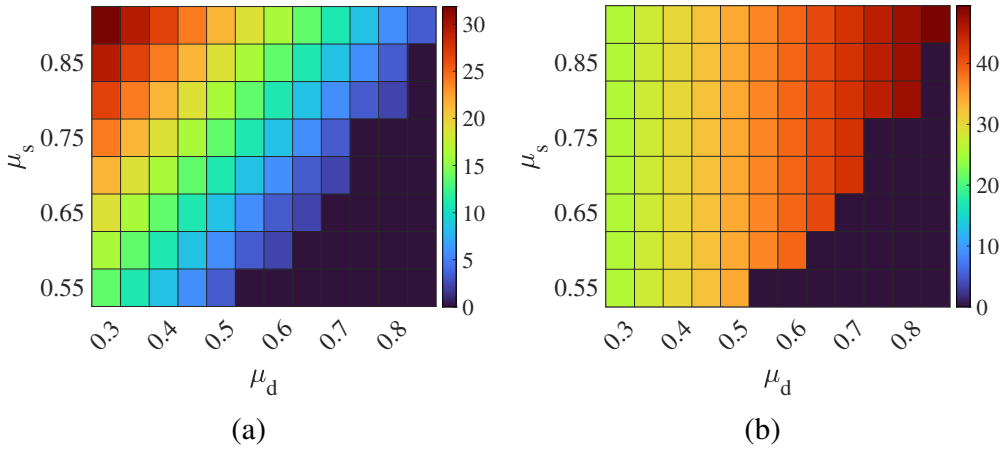

(a) (b)

Figure 6.2: The maximum body jerk at (a) start and (b) stop, for different values of μ_s and μ_d.

6.2.2 Experimental Observation of Jerk Peaks

To examine whether similar behavior occurs in a real vehicle, experimental tests were conducted and analyzed. Figure 6.3 [20] shows the measured body jerk during a

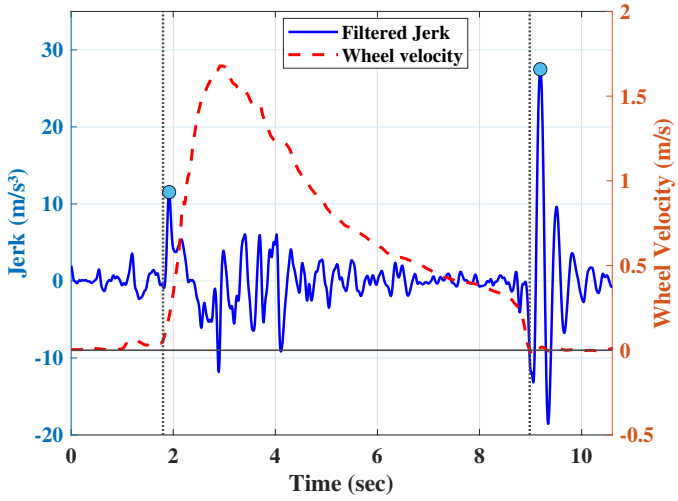

Figure 6.3: Jerk of vehicle body found in experiments.

low-speed start and stop manoeuvre.

The experimental results show distinct jerk peaks during both motion initiation and braking. In both cases, the jerk peaks occur close to the transitions between motion and standstill. The two marked points in Fig. 6.3 indicate the maximum jerk magnitudes associated with the start and stop events.

6.2.3 Phase-Space Representation of Relative Motion

To relate the measured jerk behavior to the relative motion between the vehicle body and the wheel, phase-space representations are examined. Figure 6.4 [20] shows the phase portraits of relative velocity versus relative displacement during the start and stop events. These phase portraits are obtained from experimental measurements after pre-processing the data and state estimation. The measured acceleration and wheel speed signals are first filtered, after which a Kalman filter is applied to estimate the system states required to construct the phase-space trajectories.

The phase portraits reveal distinct trajectory patterns for the two manoeuvres. During start, the trajectory exhibits dispersed loops before converging, whereas during stop the trajectory follows a clear inward spiral toward an equilibrium point.

6.2.4 Non-smooth Behavior Near Standstill

Figure 6.5(a) [19] shows the wheel velocity for selected braking cases. In some cases, the wheel velocity reaches zero and subsequently reverses direction before finally stopping.

To analyze this behavior, further investigation of the non-smooth dynamics was

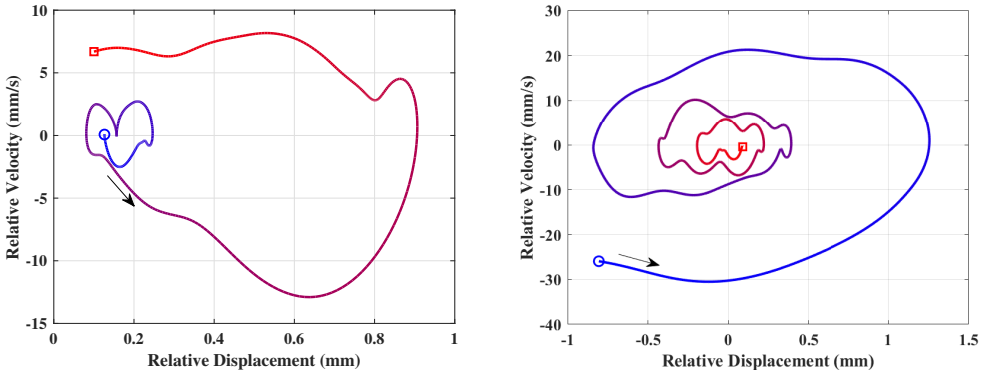

(a) (b)

Figure 6.4: Phase portrait for relative velocity and displacement: (a) at start and (b) at stop from test.

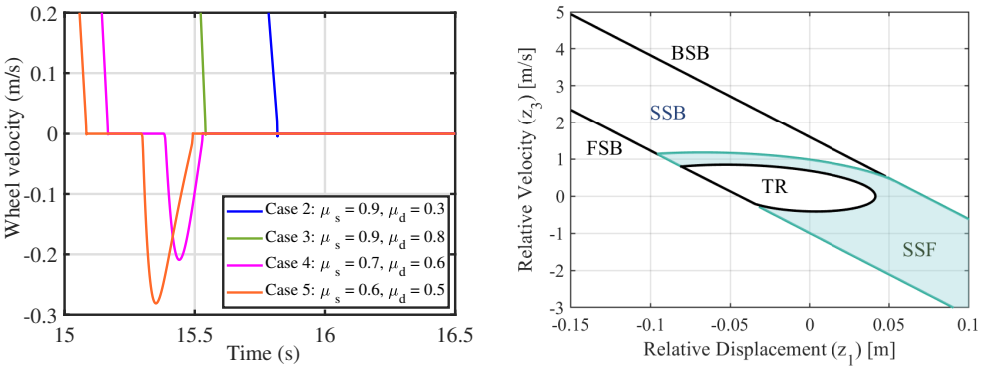

(a) (b)

Figure 6.5: (a) Different wheel speeds cases, and (b) Trapping and stick-slip regions.

performed. Figure 6.5(b), taken from [21], shows the trapping and stick–slip regions in the phase space. The trapping region (TR) corresponds to conditions under which the wheel remains stuck and trajectories converge toward a sticking equilibrium. The regions SSF (stick–slip forward) and SSB (stick–slip backward) represent conditions under which trajectories may leave the sticking regime and the wheel begins to move. The boundaries FSB and BSB denote the forward and backward slip boundaries separating the sticking regime from the corresponding rolling directions. These regions provide a qualitative interpretation of whether the system returns to sticking or transitions into moving.

Chapter 7

Discussion and Conclusion

This chapter discusses the results presented in Chapter 6. The discussion links the numerical and experimental observations to the modeling assumptions and research questions of the thesis, followed by a concluding summary and directions for future work.

7.1 Discussion

The results demonstrate that low-speed start and stop manoeuvres are characterized by pronounced transient behavior. Both numerical simulations and experimental measurements consistently show sharp jerk peaks near motion initiation and near standstill, confirming that low-speed operation is particularly sensitive to non-smooth effects.

The numerical results obtained from the minimal longitudinal vehicle model reveal distinct sensitivities to the static and dynamic brake friction coefficients during start and stop manoeuvres [19]. During vehicle start, the magnitude of the jerk peak is strongly governed by the transition from static to dynamic friction. In particular, a larger friction contrast $\Delta\mu = \mu_s - \mu_d$ produces a stronger force discontinuity at the onset of motion and therefore increases the resulting jerk peak. Consequently, a large static friction coefficient combined with a smaller dynamic friction coefficient results in a more abrupt force release during start, leading to elevated jerk levels and reduced comfort.

In contrast, the stopping behavior is primarily influenced by the dynamic friction coefficient. For a given value of dynamic friction coefficient μ_d, variations in the static friction coefficient μ_s have only a minor effect on the jerk response. Overall, higher values of μ_d lead to increased jerk and reduced comfort during braking, largely independent of μ_s. Moreover, a smaller separation between the friction coefficients, quantified by a reduced $\Delta\mu$, results in more pronounced oscillations near standstill. These observations indicate that discomfort during stopping is mainly governed by

dynamic friction properties and their interaction with non-smooth braking dynamics.

These trends observed in simulation are further supported by experimental measurements from a real vehicle [20]. The measured body jerk exhibits clear and repeatable peaks during both start and stop events, occurring close to the transitions between motion and rest. Although the experimental data contain additional variability due to measurement noise and unmodeled effects, the timing and qualitative characteristics of the jerk response are consistent with the results obtained from the minimal longitudinal vehicle model. This agreement confirms that the minimal longitudinal model captures the dominant low-speed dynamics relevant to jerk generation.

Phase-space representations provide further insight into the underlying mechanisms governing this behavior [20]. During stop manoeuvres, both simulation and experimental phase portraits show trajectories that converge smoothly toward an equilibrium point, which is characteristic of a damped system approaching rest under the combined influence of braking friction and suspension compliance. This behavior is clearly visible in Fig. 6.4(b), where the inward spiraling trajectory indicates stable convergence near standstill. In contrast, start manoeuvres exhibit more dispersed trajectories with repeated loops in phase space, reflecting repeated transitions between static and dynamic friction. This asymmetry between start and stop dynamics explains why the two manoeuvres exhibit different jerk characteristics and highlights the critical role of friction-induced non-smooth transitions at low speeds.

An important observation emerges from the analysis of wheel velocity behavior near standstill [19]. In certain braking scenarios, the wheel velocity reaches zero and subsequently reverses direction before finally settling, a phenomenon that cannot be explained by smooth or purely continuous models. This behavior is a direct consequence of non-smooth friction dynamics and the associated stick–slip transitions. The phase-space analysis reveals the existence of distinct trapping and stick–slip regions that govern the system's response [21]. Trajectories originating outside the trapping region are associated with higher peak jerk values and sharp discontinuities caused by repeated transitions between sticking and sliding. In contrast, trajectories that enter the trapping region exhibit smoother jerk evolution, lower peak values, and stable convergence to rest.

Within the stick–slip regions, the system response depends on both the road slope and the specific location in phase space [21]. In downhill scenarios, trajectories entering the stick–slip forward (SSF) region and exiting through the forward slip boundary (FSB) are not sufficiently counteracted by friction, preventing the system from returning to rest and leading to continued acceleration. Conversely, trajectories originating in the stick–slip backward (SSB) region may undergo brief slipping but can re-enter the sticking region, transition into the trapping region, and ultimately come to a complete stop. Taken together, these results highlight the importance of identifying and guiding the system into the trapping region during braking, both to minimize jerk-related discomfort and to ensure stable stopping behavior. More broadly, this analysis demonstrates that low-

speed braking must be treated as a non-smooth dynamical system, rather than relying solely on continuous approximations, in order to capture the mechanisms underlying discomfort and instability near standstill.

7.2 Conclusions and Future Work

This thesis investigated low-speed longitudinal vehicle dynamics with a focus on brake-friction effects, jerk generation, and non-smooth behavior during start and stop manoeuvres. The first research question examined whether a minimal longitudinal model can represent the oscillation and jerk phenomena observed in real world. The results show that, despite its low complexity, the proposed model captures the dominant transient behavior observed in real-world vehicle measurements. In particular, the model reproduces the characteristic jerk peaks at the onset of motion and during braking, and it provides a mechanistic explanation for how these peaks arise from brake-friction transitions combined with longitudinal compliance. Comparisons with CarMaker further showed that the minimal model captures the overall low-speed velocity and acceleration profiles well. The experimental results further supported these findings by confirming pronounced jerk peaks during both start and stop manoeuvres, occurring close to transitions between motion and standstill. Moreover, the estimated phase-space trajectories exhibited characteristic start–stop patterns consistent with the non-smooth behavior predicted by the minimal model.

The second research question addressed whether a mathematical and computational framework can be formulated that accounts for the non-smooth characteristics of brake friction while still producing robust simulation results. This thesis demonstrated that a Filippov-based formulation combined with event-driven integration provides a consistent and numerically stable representation of switching dynamics at zero velocity. A friction state machine and event detection were introduced to handle transitions between sticking and sliding without numerical chattering, enabling stable simulation of repeated stick–slip transitions.

Overall, the thesis shows that combining a minimal model, a non-smooth dynamical systems formulation, and an event-driven numerical scheme yields a physically interpretable and computationally efficient framework for studying jerk and comfort in low-speed start and stop manoeuvres. The results highlight brake-friction transitions as an important factor behind discomfort near standstill.

Although the current model captures key low-speed phenomena, several natural extensions remain. An important next step is the inclusion of road–tire friction, which would allow the framework to account for surface-dependent effects and varying grip conditions. Further development of tire models, including longitudinal compliance and more detailed force generation, would improve the representation of wheel behavior near standstill. From an application perspective, extending the framework to heavier vehicles

such as trucks is a promising direction, where low-speed comfort and braking behavior are particularly challenging. Ongoing and future collaboration with industry provides an opportunity to validate and apply the proposed methods to industrial vehicle platforms and real-world scenarios. In addition, the insights gained in this thesis form a strong basis for future control-oriented developments, where low-speed control strategies explicitly account for non-smooth friction dynamics in order to reduce jerk and improve ride comfort.

Bibliography

[1] K. N. de Winkel, F. Soyka, and H. H. Bulthoff. The role of acceleration and jerk in perception of above-threshold surge motion. In: *Experimental Brain Research* 238.3 (2020), pp. 699–711.

[2] K. N. De Winkel, T. Irmak, R. Happee, and B. Shyrokau. Standards for passenger comfort in automated vehicles: Acceleration and jerk. In: *Applied Ergonomics* 106 (2023), p. 103881.

[3] F. Walz and S. Hohmann. Model predictive longitudinal motion control for low velocities on known road profiles. In: *Vehicle System Dynamics* 58.8 (2020), pp. 1310–1328.

[4] S. Das and S. Shrudhanidhi. Vehicle Dynamics Modelling: Lateral and Longitudinal. In: *2021 8th International Conference on Signal Processing and Integrated Networks (SPIN)*. IEEE. 2021, pp. 407–412.

[5] I. Blekhman and E. Kremer. Vertical-longitudinal dynamics of vehicle on road with unevenness. In: *Procedia Engineering* 199 (2017), pp. 3278–3283.

[6] Z. Guo, W. Wu, and S. Yuan. Longitudinal-vertical dynamics of wheeled vehicle under off-road conditions. In: *Vehicle System Dynamics* 60.2 (2022), pp. 470–490.

[7] M. Marcano, J. A. Matute, R. Lattarulo, E. Martí, and J. Pérez. Low speed longitudinal control algorithms for automated vehicles in simulation and real platforms. In: *Complexity* 2018.1 (2018), p. 7615123.

[8] S. Ye, J. Lu, H. Wei, H. Lu, L. Shi, and B. Wu. Analysis of transient longitudinal dynamic behavior of tire on μ-step road. In: *Proceedings of the Institution of Mechanical Engineers, Part D: Journal of Automobile Engineering* 237.8 (2023), pp. 1914–1928.

[9] M. Bernardo, C. Budd, A. R. Champneys, and P. Kowalczyk. Piecewise-smooth dynamical systems: theory and applications. Vol. 163. Springer Science & Business Media, 2008.

[10] A. F. Filippov. Differential equations with discontinuous righthand sides: control systems. Vol. 18. Springer Science & Business Media, 2013.

[11] P. T. Piiroinen and Y. A. Kuznetsov. An event-driven method to simulate Filippov systems with accurate computing of sliding motions. In: *ACM Transactions on Mathematical Software (TOMS)* 34.3 (2008), pp. 1–24.

[12] H. Koylu and E. Tural. Experimental study on braking and stability performance during low speed braking with ABS under critical road conditions. In: *Engineering Science and Technology, an International Journal* 24.5 (2021), pp. 1224–1238.

[13] Z. Chen, R. Xiong, X. Cai, Z. Wang, and R. Yang. Regenerative braking control strategy for distributed drive electric vehicles based on slope and mass coestimation. In: *IEEE Transactions on Intelligent Transportation Systems* 24.12 (2023), pp. 14610–14619.

[14] P. Fajri, S. Heydari, and N. Lotfi. Optimum low speed control of regenerative braking for electric vehicles. In: *2017 IEEE 6th International conference on renewable energy research and applications (ICRERA)*. IEEE. 2017, pp. 875–879.

[15] J. Lee and S. Choi. Braking control for improving ride comfort. In: *MATEC Web of Conferences*. Vol. 166. EDP Sciences. 2018, p. 02002.

[16] A. Singh and O. Nishihara. Modeling of autonomous emergency braking system with minimum jerk. In: *2022 22nd international conference on control, automation and systems (ICCAS)*. IEEE. 2022, pp. 40–44.

[17] E. Pennestri, V. Rossi, P. Salvini, and P. P. Valentini. Review and comparison of dry friction force models. In: *Nonlinear dynamics* 83.4 (2016), pp. 1785–1801.

[18] H. Olsson. Control of Systems with Friction. PhD thesis. Lund, Sweden: Department of Automatic Control, Lund Institute of Technology, 1996.

[19] S. Deylaghian, M. Jonasson, and P. T. Piiroinen. A Comparative Study of Discomfort Using Electrical and Friction Braking at Low Speed Driving. In: *Advanced Vehicle Control Symposium*. Springer. 2024, pp. 714–720.

[20] S. Deylaghian, M. Jonasson, and P. T. Piiroinen. State estimation and characterization of longitudinal vehicle dynamics at low speeds using experimental data. In: *IAVSD Symposium on the Dynamics of Vehicles on Roads and on Tracks*. Springer. 2025.

[21] S. Deylaghian, P. T. Piiroinen, and M. Jonasson. Locating Trapping Regions and Analyzing Jerk in a Minimal Vehicle Model. In: *Submitted to International Journal of Non-Linear Mechanics* (2026).

[22] V. I. Utkin. Sliding modes in control and optimization. Springer Science & Business Media, 2013.

[23] 221e S.r.l. Muse: Miniaturized Multi-Sensor IMU. Product Datasheet A3b1v03 / A3b2v03. 221e S.r.l., 2022. URL: https://www.221e.com/muse-miniaturized-multi-sensor-imu.

[24] M. Shouran and E. Elgamli. Design and implementation of Butterworth filter. In: *Int. J. Innov. Res. Sci. Eng. Technol* 9.9 (2020), pp. 7975–7983.

[25] K. Hirano, S. Nishimura, and S. Mitra. Design of digital notch filters. In: *IEEE Transactions on Communications* 22.7 (1974), pp. 964–970.

[26] C. K. Chui and G. Chen. Kalman filtering: with real-time applications. Springer, 2009.

[27] IPG Automotive GmbH. CarMaker – Vehicle Dynamics Simulation. https://ipg-automotive.com/products/carmaker/. Accessed: 2026-02-06.